JACS
JOURNAL OF THE AMERICAN CHEMICAL SOCIETY
Communication
pubs.acs.org/JACS

Shaping of Metal–Organic Frameworks: From Fluid to Shaped Bodies and Robust Foams

Yifa Chen,[†] Xianqiang Huang,[‡] Shenghan Zhang,[†] Siqing Li,[†] Sijia Cao,[†] Xiaokun Pei,[†] Junwen Zhou,[†] Xiao Feng,[†] and Bo Wang*[,†]

[†]Key Laboratory of Cluster Science, Ministry of Education of China, School of Chemistry, Beijing Institute of Technology, 5 South Zhongguancun Street, Beijing, 100081, P. R. China

[‡]Shandong Provincial Key Laboratory of Chemical Energy Storage and Novel Cell Technology, School of Chemistry & Chemical Engineering, Liaocheng University, Liaocheng, 252059, P. R. China

Supporting Information

ABSTRACT: The applications of metal–organic frameworks (MOFs) toward industrial separation, catalysis, sensing, and some sophisticated devices are drastically affected by their intrinsic fragility and poor processability. Unlike organic polymers, MOF crystals are insoluble in any solvents and are usually not thermoplastic, which means traditional solvent- or melting-based processing techniques are not applicable for MOFs. Herein, a continuous phase transformation processing strategy is proposed for fabricating and shaping MOFs into processable fluids, shaped bodies, and even MOF foams that are capable of reversible transformation among these states. Based on this strategy, a cup-shaped Cu-MOF composite and hierarchically porous MOF foam were developed for highly efficient catalytic C–H oxidation (conv. 76% and sele. 93% for cup-shaped Cu-MOF composite and conv. 92% and sele. 97% for porous foam) with ease of recycling and dramatically improved kinetics. Furthermore, various MOF-based foams with low densities (<0.1 g cm^{-3}) and high MOF loadings (up to 80 wt %) were obtained via this protocol. Imparted with hierarchically porous structures and fully accessible MOFs uniformly distributed, these foams presented low energy penalty (pressure drop <20 Pa, at 500 mL min^{-1}) and showed potential applications as efficient membrane reactors.

By virtue of their structural periodicity and tunability, high porosity, and rich functionality, metal–organic frameworks (MOFs) are of great interest and show potential in many important applications such as gas storage/separation, sensing, drug delivery, and catalysis.[1] However, MOF crystals are often brittle and can easily break into tiny particles or fine powders. Furthermore, MOFs, unlike organic polymers, tend to be insoluble in any solvents and are usually not thermoplastic. All these dampen MOFs' processability and hamper their further industrial applications. For instance, catalysis using MOF crystals can be severely affected by catalyst loss and pipe clog that will inevitably occur when flushing with fluids (e.g., gas or liquid) during catalytic cycles. Hence, new methods for fabricating and shaping porous crystalline solids, like MOFs, into processable fluids, shaped bodies, and even foams are highly desirable.[2]

General processing methods for MOFs include pressing or extrusion under high pressure with/without binders and additives.[3] The obtained materials (e.g., beads, pellets, etc.) with inactive ingredients and/or binders blocking the pores often show lower porosity and diminished catalytic activity. Some interesting MOF-based porous composites with accessible porosity were reported[4] and were mostly achieved via two major methods: (1) *in situ* growth of MOFs on porous substrates (e.g., silica aerogel and polyHIPE foam, etc.) through approaches such as seeding growth, Layer-by-Layer (LBL) deposition, hydrothermal, and so on;[5] (2) post-treatment strategies conducted via the combination of preformed MOFs with other additives followed with special treatments (microwave-assisted polymerization, sol–gel casting, freeze-drying and surfactant-assisted dip-coating, etc.).[6]

Overall, these studies, while encouraging, were limited in certain MOF systems with relatively low MOF loadings (usually lower than 30%) and lack of mechanical stability. Besides, systemic investigation of MOFs into various phases and/or morphologies (e.g., liquid, gel, foam, film, etc.) during the shaping of MOFs was rarely reported. Herein, we embarked on exploring the possibilities of MOF shaping, from crystalline solids to transformable fluids, gels, and further into robust shaped bodies and foams. We presented a strategy for the continuous and reversible processing of MOF-based materials and successfully applied it into various MOFs. Specifically, by introducing HKUST-1@Fe_3O_4 core–shell nanoparticles into carboxymethylcellulose (CMC) solution, we have achieved magnetic fluid (denoted as HKUST-1@Fe_3O_4-MF) with high particle contents (25.0 to 45.4 wt %). Based on this magnetic fluid, a cup reactor was fabricated with a solvent-induced hardening process. Moreover, a light and robust foam with hierarchical porosity was obtained by freeze-drying of HKUST-1@Fe_3O_4-MF for efficient C–H oxidation (Scheme 1a). To study the feasibility of this strategy, we further synthesized a variety of foams from several important and distinct MOFs with high MOF loadings and low pressure resistance (Scheme 1b).

Received: July 6, 2016
Published: August 11, 2016

DOI: 10.1021/jacs.6b06959
J. Am. Chem. Soc. 2016, 138, 10810–10813

Scheme 1. (a) Schematic Procedure of HKUST-1@Fe_3O_4-MF and the Transformation from Magnetic Fluid to Gel, Shaped Bodies and a Porous Foam; (b) Other Foams Derived from Representative MOFs Achieved Using This Strategy

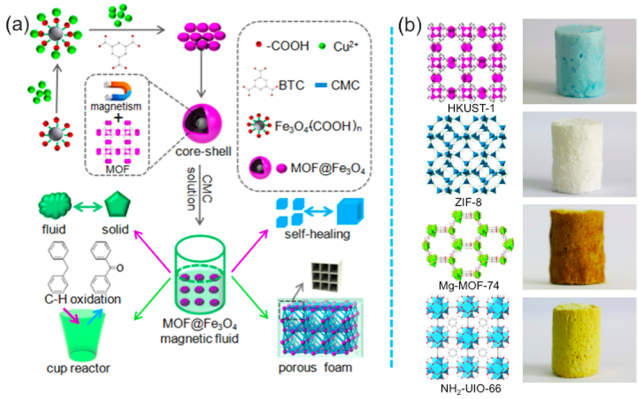

The preparation of HKUST-1@Fe_3O_4-MF is illustrated in Scheme 1a. First, core−shell HKUST-1@Fe_3O_4 nanoparticles (~100 nm) were prepared through a secondary-growth approach according to our previous report.[7] Second, the obtained nanoparticles were predispersed in acetone by ultrasound[8] and then added into an as-prepared transparent CMC aqueous solution followed by high-speed mechanical stirring. Flowable HKUST-1@Fe_3O_4-MF, which could be drawn toward a magnet, was obtained (Figure 1a). The powder X-ray diffraction (PXRD) pattern demonstrates that the underlying topology of HKUST-1 is retained (Figure S2b). Scanning electron microscopy (SEM) and energy dispersive X-ray spectroscopy (EDS) mapping reveal uniform dispersion of HKUST-1@Fe_3O_4 in the fluid (Figure S2c,d).

Remarkably, HKUST-1@Fe_3O_4-MF is imparted with phase transition ability to reversibly transform from fluid to gel and to the solid state. Upon immersing in a small amount of CH_3CN ($V(CH_3CN)/V(MF)$ = 1/10) for 10 min, the fluid was converted to a gel state (HKUST-1@Fe_3O_4-gel), in which the material is soft yet loses its fluidity. It is worth noting that the thus-obtained gel exhibits self-healing ability.[9] Four pieces cut from a bulk of gel could be gathered together to reform the bulk material in just 5 min by using a magnet (Figure 1b). The gel material can be further converted to the solid state by soaking it in five times its volume of CH_3CN. Using this method, the magnetic fluid is capable of shaping into the desired form with a mold, such as bulk material and even stand-alone film (Figure 1a,c and Figure S4). Moreover, these shaped bodies are able to reconvert to gel and even to the fluid state upon adding different amounts of water.

Specially, we fabricated a cup reactor through solidification of HKUST-1@Fe_3O_4-MF (40 wt %, Figure 1c) and then applied it for C−H activation catalysis without using any extra catalyst (Figure 1e). SEM image and EDS mapping of the inner side of the cup indicate uniform dispersion of HKUST-1@Fe_3O_4 (Figures 1d and S5). Diphenylmethane (0.250 mmol), *tert*-butyl hydroperoxide (0.625 mmol), and chlorobenzene (2 mL) were premixed and added to the cup reactor. The cup reactor was subsequently heated at 60 °C in an oven for 24 h (a cover was put on top of the cup), and conv. 76% and sele. 93% was achieved (Figure 1e,f). The product allows ease of collection by pouring out without the need for separation of the catalyst. It should be noted that the cup reactor could be directly used for

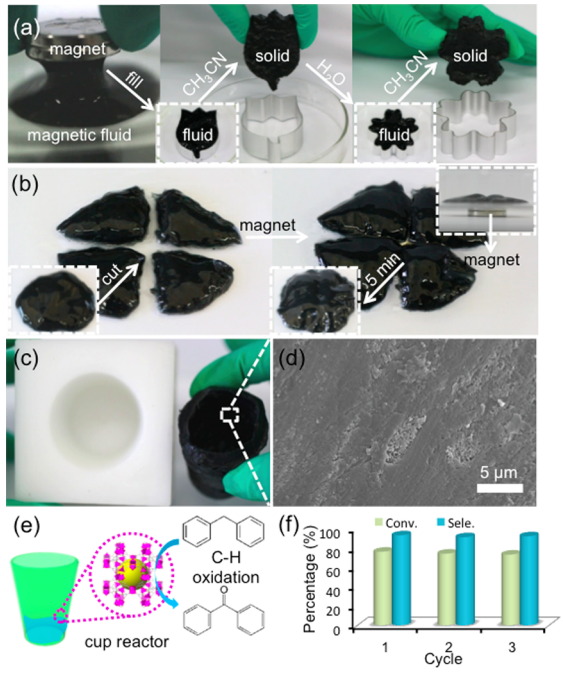

Figure 1. (a) Photo images of reversible phase transformation. From left to right: the fluid that could be drawn toward a magnet was filled in a tulip-shape mold followed by immersing in CH_3CN, and then a tulip-shape bulk material was obtained. The bulk material turned back to fluid after treating in water, and then it was converted to a sakura-shape bulk material upon CH_3CN treating. (b) Self-healing property of the HKUST-1@Fe_3O_4-gel. (c) A cup reactor prepared by solvent-inducing approach. (d) SEM image of the inner surface of the cup reactor. (e) Schematic representation of the cup reactor for C−H oxidation catalysis. (f) Catalytic performance of the cup reactor.

the next catalytic cycle, and the activity and stability of the cup reactor were still retained after three cycles (Figures 1f and S6).

To further explore the catalytic performances of other MOF-based shaped bodies, we also fabricated robust foams. We attempted to directly freeze-dry HKUST-1@Fe_3O_4-MF to generate hierarchical porosity. After freeze-drying of the fluids in a cylinder shaped mold, light foams with different densities (0.058 to 0.072 g cm^{-3}) were obtained by varying the loadings of HKUST-1@Fe_3O_4 (Figures S7a and S8). Using the foam with 40 wt % for example, the PXRD pattern indicates the retained phase of HKUST-1@Fe_3O_4 (Figure S9). Based on the N_2 sorption isotherms at 77 K, the surface area (S_{BET}) of this foam is 196 m^2 g^{-1} and the pore volume is 0.65 cm^3 g^{-1} (Figure S7b and Table S1). Quenched solid-state density functional theory (QSDFT) calculation reveals the foam possesses hierarchically distributed porosity with a pore size distribution in both the micro- and mesopore range (up to 40 nm). In comparison, CMC foam prepared under similar conditions shows an S_{BET} of 24 m^2 g^{-1} and a mesopore size distribution (up to 10 nm) with a pore volume of 0.06 cm^3 g^{-1} (Table S1). The porosity of the foam was also verified by CO_2 adsorption (60 cm^3 g^{-1}, 273 K and 45 cm^3 g^{-1}, 298 K, Figure S10). As shown in the SEM image, this foam presents cell-like structure with macropores in the micrometer range (Figures S7c and S11). The above results demonstrate hierarchical porosities were successfully generated in the foam by the freeze-drying approach. Besides, this foam with low density and magnetism can be readily attracted by a magnet (Figure S7e). As proven by a magnetism test at 298 K, the magnetization saturation values

DOI: 10.1021/jacs.6b06959
J. Am. Chem. Soc. 2016, 138, 10810−10813

of the foams (25.0 to 45.4 wt %) at 10 T were measured to be 0.15 to 0.43 emu g^{-1}, respectively (Figure S7f).

Robustness is one of the critical prerequisites in practical applications, as it determines the durability of materials especially under harsh conditions. Proven by weight pressing, tape test, and collision experiment, this foam possesses extraordinary mechanical stability and robustness (Figure 2a,c,d). In contrast, the CMC foam shrunk to 20% of its

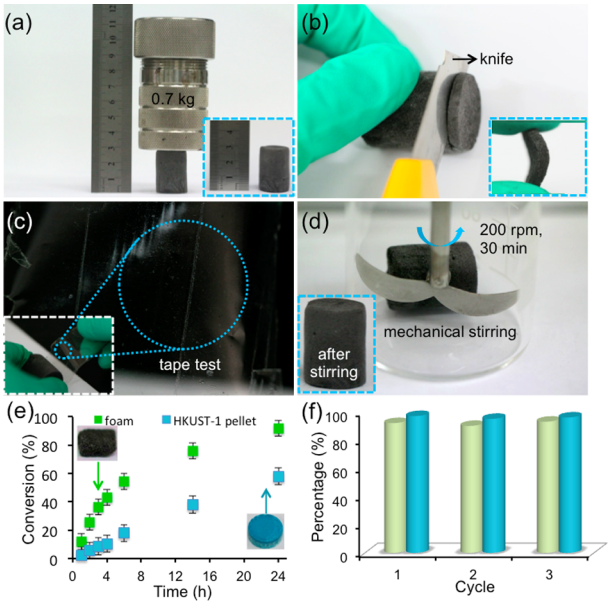

Figure 2. (a) Pressing experiment of the HKUST-1@Fe_3O_4-foam (40 wt %) conducted with an autoclave, insert image presents the state before pressing. (b) Foam cut into thin films with a knife; insert is the obtained film that can tolerant bending. (c) The surface of the Scotch Tape after tape test. (d) Mechanical stability test of the foam. (e) Kinetic catalysis performance of the foam and HKUST-1 pellet (pressing at 10 MPa, 5 wt % sesbania gum powder as auxiliary agent). (f) Recycle performances of the foam (green, conversion and cyan, selectivity).

original volume under pressing (Figure S12). Furthermore, HKUST-1@Fe_3O_4-foam can be cut into a stand-alone thin film that is able to tolerate bending (Figure 2b).

Given the excellent robustness and processing properties of the foam, we further set out to explore its applications in catalysis. This foam possesses extraordinary performance (conv. 92% and sele. 97%) in the catalysis of C−H oxidation (Figure 2f). It also shows a higher reaction rate than the simulated industrial pressing HKUST-1 pellet with similar MOF content as in the foam (conv. 58% and sele. 98%) (Figure 2e).[10] After catalysis, HKUST-1@Fe_3O_4-foam could be readily recycled three times without losing its activity (Figure 2f and Figure S13).

Furthermore, we successfully extended this protocol to several representative MOFs. Specifically, six MOFs with distinct metal clusters, organic linkers, topologies, and/or functionalities were synthesized and successfully fabricated into robust foams under the same procedures (Figures 3 and S15).[11] The underlying topologies of these MOFs were retained after processing into foams proven by PXRD tests (Figures S16−21). As presented in Figure 3, these foams all presented cellular textures with macropores in the micrometer range. MOF particles were uniformly distributed inside these foams as

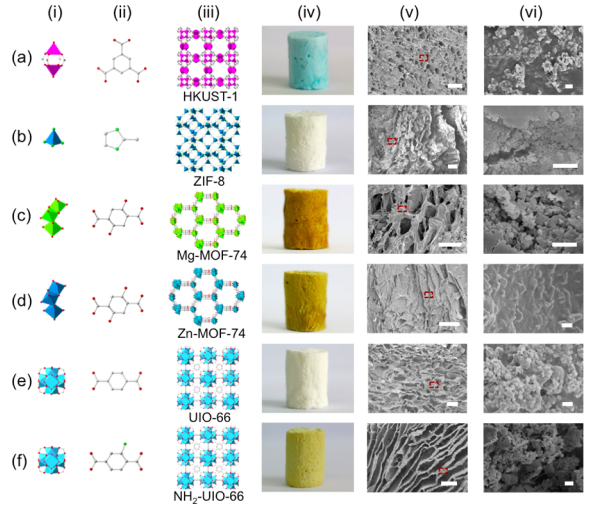

Figure 3. (a) HKUST-1@CMC-foam (40 wt %). (b) ZIF-8@CMC-foam (40 wt %). (c) Mg-MOF-74@CMC-foam (40 wt %). (d) Zn-MOF-74@CMC-foam (40 wt %). (e) UIO-66@CMC-foam (40 wt %). (f) NH_2-UIO-66@CMC-foam (40 wt %). Metal clusters (i), linkers (ii), and the structures (iii) are presented for the corresponding MOFs. Atoms: Cu, pink; Zn, dark cyan; Mg, light green; Zr, blue; N, green and O, red. Photo images (iv) and SEM images (v, vi) of the prepared foams; vi is the zoomed-in image of the square box in v. The scale bars are 100 μm in v and 1 μm in vi.

shown by SEM and EDS mapping analyses (Figures S22−27). By virtue of these unique hierarchical porous structures, these MOF foams were light in weight and the volume densities were all below 0.1 g cm^{-3} (Table S2). Besides, these foams exhibited low pressure resistance. In a pressure resistance test, MOF films (2.5 cm, diameter and 4 mm, thickness) cut from the pristine foams showed a low pressure drop (<20 Pa) in a gas flow rate of 500 mL min^{-1} (Figure S28). Importantly these MOF foams with extremely high MOF loadings were also investigated. Processed under the same protocol, ZIF-8@CMC-foam (80 wt %) with low density (0.094 g cm^{-3}) was achieved (Figure S29) which was among the highest values reported.[8]

In conclusion, we incorporated HKUST-1@Fe_3O_4 nanoparticles and CMC to form magnetic fluid and presented a facile strategy to transform this fluid to gel and shaped bodies. The successful transformation among these states with good reversibility by the solvent-inducing method imparts this MOF-based composite with great processability and recoverability. Specially, we prepared a cup reactor to catalyze the C−H oxidation reaction (conv. 76% and sele. 93%). To further improve the catalytic efficiency and develop more practical catalyst shaped bodies for industrial application, we directly freeze-dried HKUST-1@Fe_3O_4-MF to yield foams with low densities, hierarchical porosities, excellent robustness, and catalytic performances. Furthermore, six unique and robust MOF foams with low densities (<0.1 g cm^{-3}) were obtained using the same protocol. The MOF loading can even reach up to 80 wt % without sacrificing the mechanical stability. And by virtue of the hierarchically porous structures and uniformly distributed MOFs, these MOF foams presented high permeability with a low pressure drop (<20 Pa, 500 mL min^{-1}) and can potentially be used as membrane reactors in various important catalytic and separation processes. It may also shed light on the exploration of porous solids, such as MOFs, COFs (covalent−organic frameworks),[12] and CMPs

DOI: 10.1021/jacs.6b06959
J. Am. Chem. Soc. 2016, 138, 10810−10813

(conjugated microporous polymers)[13] toward many industrial applications.

■ ASSOCIATED CONTENT

Supporting Information

The Supporting Information is available free of charge on the ACS Publications website at DOI: 10.1021/jacs.6b06959.

Experimental details and additional characterizations (PDF)

■ AUTHOR INFORMATION

Corresponding Author

*bowang@bit.edu.cn

Notes

The authors declare no competing financial interest.

■ ACKNOWLEDGMENTS

This work was financially supported by the 973 Program 2013CB834704; Provincial Key Project of China (Grant No. 7131253); the National Natural Science Foundation of China (Grant Nos. 21471018, 21404010, 21201018, 21490570, 21401094); and 1000 Plan (Youth).

■ REFERENCES

(1) (a) Li, H.; Eddaoudi, M.; O'Keeffe, M.; Yaghi, O. M. *Nature* **1999**, *402*, 276. (b) Kitaura, R.; Kitagawa, S.; Kubota, Y.; Kobayashi, T. C.; Kindo, K.; Mita, Y.; Matsuo, A.; Kobayashi, M.; Chang, H. C.; Ozawa, T. C.; Suzuki, M.; Sakata, M.; Takata, M. *Science* **2002**, *298*, 2358. (c) Ferey, G.; Mellot-Draznieks, C.; Serre, C.; Millange, F.; Dutour, J.; Surble, S.; Margiolaki, I. *Science* **2005**, *309*, 2040. (d) Shekhah, O.; Belmabkhout, Y.; Chen, Z.; Guillerm, V.; Cairns, A.; Adil, K.; Eddaoudi, M. *Nat. Commun.* **2014**, *5*, 10.1038/ncomms5228. (e) He, C. T.; Jiang, L.; Ye, Z. M.; Krishna, R.; Zhong, Z. S.; Liao, P. Q.; Xu, Q.; Ouyang, F.; Zhang, J. P.; Chen, X. M. *J. Am. Chem. Soc.* **2015**, *137*, 7217.

(2) (a) Czaja, A. U.; Trukhan, N.; Muller, U. *Chem. Soc. Rev.* **2009**, *38*, 1284. (b) Chen, Y.; Li, S.; Pei, X.; Zhou, J.; Feng, X.; Zhang, S.; Cheng, Y.; Li, H.; Han, R.; Wang, B. *Angew. Chem., Int. Ed.* **2016**, *55*, 3419.

(3) (a) Blanita, G.; Coldea, L.; Misan, L.; Lupu, D. *Int. J. Hydrogen Energy* **2014**, *39*, 17040. (b) Hong, W. Y.; Perera, S. P.; Burrows, A. D. *Microporous Mesoporous Mater.* **2015**, *214*, 149. (c) O'Neill, L. D.; Zhang, H. F.; Bradshaw, D. *J. Mater. Chem.* **2010**, *20*, 5720. (d) Zacharia, R.; Cossement, D.; Lafi, L.; Chahine, R. *J. Mater. Chem.* **2010**, *20*, 2145.

(4) (a) Zhu, Q. L.; Xu, Q. *Chem. Soc. Rev.* **2014**, *43*, 5468. (b) Yusuf, K.; Badjah-Hadj-Ahmed, A. Y.; Aqel, A.; ALOthman, Z. A. *J. Chromatogr. A* **2015**, *1406*, 299. (c) Wickenheisser, M.; Paul, T.; Janiak, C. *Microporous Mesoporous Mater.* **2016**, *220*, 258. (d) Lyu, D. Y.; Yang, C. X.; Yan, X. P. *J. Chromatogr. A* **2015**, *1393*, 1.

(5) (a) Shekhah, O.; Fu, L. L.; Sougrat, R.; Belmabkhout, Y.; Cairns, A. J.; Giannelis, E. P.; Eddaoudi, M. *Chem. Commun.* **2012**, *48*, 11434. (b) Ramos-Fernandez, E. V.; Garcia-Domingos, M.; Juan-Alcaniz, J.; Gascon, J.; Kapteijn, F. *Appl. Catal., A* **2011**, *391*, 261. (c) Hu, Y. L.; Lian, H. X.; Zhou, L. J.; Li, G. K. *Anal. Chem.* **2015**, *87*, 406.

(6) (a) Ulker, Z.; Erucar, I.; Keskin, S.; Erkey, C. *Microporous Mesoporous Mater.* **2013**, *170*, 352. (b) Li, L.; Xiang, S. L.; Cao, S. Q.; Zhang, J. Y.; Ouyang, G. F.; Chen, L. P.; Su, C. Y. *Nat. Commun.* **2013**, *4*, 10.1038/ncomms2757. (c) Lin, K. Y. A.; Chang, H. A. *J. Mater. Chem. A* **2015**, *3*, 20060. (d) Lin, C. L.; Lirio, S.; Chen, Y. T.; Lin, C. H.; Huang, H. Y. *Chem. - Eur. J.* **2014**, *20*, 3317. (e) Zhu, H.; Yang, X.; Cranston, E. D.; Zhu, S. P. *Adv. Mater.* **2016**, DOI: 10.1002/adma.201601351.

(7) Chen, Y. F.; Huang, X. Q.; Feng, X.; Li, J. K.; Huang, Y. Y.; Zhao, J. S.; Guo, Y. X.; Dong, X. M.; Han, R. D.; Qi, P. F.; Han, Y. Z.; Li, H. W.; Hu, C. W.; Wang, B. *Chem. Commun.* **2014**, *50*, 8374.

(8) Denny, M. S.; Cohen, S. M. *Angew. Chem., Int. Ed.* **2015**, *54*, 9029.

(9) Chen, X. X.; Dam, M. A.; Ono, K.; Mal, A.; Shen, H. B.; Nutt, S. R.; Sheran, K.; Wudl, F. *Science* **2002**, *295*, 1698.

(10) Leng, Y. X.; Zhang, Y.; Huang, C. X.; Liu, X. C.; Wu, Y. Z. *Bull. Korean Chem. Soc.* **2013**, *34*, 1160.

(11) (a) Schaate, A.; Roy, P.; Godt, A.; Lippke, J.; Waltz, F.; Wiebcke, M.; Behrens, P. *Chem. - Eur. J.* **2011**, *17*, 6643. (b) Bachman, J. E.; Smith, Z. P.; Li, T.; Xu, T.; Long, J. R. *Nat. Mater.* **2016**, *15*, 845. (c) Glover, T. G.; Peterson, G. W.; Schindler, B. J.; Britt, D.; Yaghi, O. M. *Chem. Eng. Sci.* **2011**, *66*, 163. (d) Cravillon, J.; Nayuk, R.; Springer, S.; Feldhoff, A.; Huber, K.; Wiebcke, M. *Chem. Mater.* **2011**, *23*, 2130. (e) Choi, K. M.; Jeong, H. M.; Park, J. H.; Zhang, Y.-B.; Kang, J. K.; Yaghi, O. M. *ACS Nano* **2014**, *8*, 7451.

(12) (a) Dalapati, S.; Addicoat, M.; Jin, S.; Sakurai, T.; Gao, J.; Xu, H.; Irle, S.; Seki, S.; Jiang, D. *Nat. Commun.* **2015**, *6*, 10.1038/ncomms8786. (b) Feng, X.; Ding, X. S.; Jiang, D. L. *Chem. Soc. Rev.* **2012**, *41*, 6010.

(13) Wu, K.; Guo, J.; Wang, C. *Angew. Chem., Int. Ed.* **2016**, *55*, 6013.

DOI: 10.1021/jacs.6b06959
J. Am. Chem. Soc. 2016, 138, 10810−10813